Lab on a Chip

Cite this: *Lab Chip*, 2012, **12**, 5218–5224

www.rsc.org/loc

PAPER

DropletMicroarray: facile formation of arrays of microdroplets and hydrogel micropads for cell screening applications†

Erica Ueda,[a] Florian L. Geyer,[ab] Victoria Nedashkivska[ab] and Pavel A. Levkin*[ab]

Received 14th August 2012, Accepted 11th October 2012
DOI: 10.1039/c2lc40921f

We describe a one-step method for creating thousands of isolated pico- to microliter-sized droplets with defined geometry and volume. Arrays of droplets are instantly formed as liquid moves along a superhydrophilic–superhydrophobic patterned surface. Bioactive molecules, nonadherent cells, or microorganisms can be trapped in the fully isolated microdroplets for high-throughput screening, or in hydrogel micropads for screening in 3D microenvironments.

Introduction

High-throughput (HT) screening of live cells is an immensely important and growing task in areas ranging from studies of gene functions using RNA interference[1] and the search for new drug candidates,[2] to screenings of new gene delivery systems[3] and the identification of factors controlling stem cell differentiation.[4] During the last decade, cell microarrays—a miniaturized method for HT cell screening—have been developed.[5–13] However, this method is limited to the transfection of adherent cells, and is unable to physically isolate one microspot from another. In addition, free diffusion of small molecules from neighboring microspots into the shared medium reduces the scope of possible applications of the cell microarrays. Thus, most cell-based screenings are still performed using either 96- or 384-well microplates. The recent emphasis on screening of nonadherent or single cells,[14] and cells in 3D microenvironments[15,16] has also encouraged the development of new screening platforms.

Droplet microfluidics-based cell culture platforms are actively progressing, and are able to address some of these issues. Cells encapsulated within picoliter- to microliter-sized droplets surrounded by an immiscible fluid, such as oil, are self-contained and can be rapidly produced (up to kHz). Positional organization of the droplets can aid in a more efficient HT screening of these droplets, especially for visualization and time-lapse measurements. However, depending on the chip design, up to 90% of the droplets may not be trapped in a microfluidic static droplet array, so precious samples could be lost, and even if the droplets are immobilized they are shown to shrink over time due to the flow of oil.[17] In addition, managing thousands of droplets in a microfluidic device can lead to complicated chip designs and many components, as well as long channels with high resistance to flow that can require higher pressures than the material can handle.[18] Another technology used to control small-scale droplet movement is digital microfluidics by electrowetting on dielectric (EWOD), which modulates the interfacial tension, using an electric field between the droplet and the underlying electrode coated with a dielectric layer. Although this method can precisely control the movement of the droplet, it requires optimization of the actuation parameters for each droplet manipulation, such as dispensing and splitting since the errors multiply with each step.[19] While microfluidics-based platforms seem promising for screens requiring many complex droplet manipulations, a simpler platform that is still capable of screening bioactive molecules, adherent cells, nonadherent cells, and cells in 3D microenvironments is desirable.

In the present work, we describe a facile one-step method for creating thousands of isolated microdroplets with defined geometry and volume, herein referred to as a Droplet Microarray. We show that the extreme wettability contrast of superhydrophilic spots on a superhydrophobic background allows spontaneous separation of an aqueous solution, leading to the formation of high-density arrays of completely separated microdroplets. This rapid and facile droplet formation does not require manual pipetting or a liquid handling device. Bioactive molecules, nonadherent cells, or microorganisms can be trapped in the fully isolated microdroplets. In this work, we also show the application of the DropletMicroarray for the preparation of a high-density array of hydrogel micropads encapsulating live cells, which can be used for HT screening of cells in 3D microenvironments.

Results and discussion

Droplet formation

To make an array of superhydrophilic spots on a superhydrophobic surface, we employed a recently published procedure

[a]*Institute of Toxicology and Genetics, Karlsruhe Institute of Technology, Postfach 3640, 76021 Karlsruhe, Germany. E-mail: levkin@kit.edu; Fax: +49 721608 29040; Tel: +49 721608 29175*
[b]*Department of Applied Physical Chemistry, Heidelberg University, 69047 Heidelberg, Germany*

† Electronic Supplementary Information (ESI) available: Details of superhydrophilic–superhydrophobic pattern preparation, microdroplet formation with methyl green solution, droplet volumes for different pattern geometries, hydrogel array images, and cell culture conditions. See DOI: 10.1039/c2lc40921f

developed in our group.[13] A 12.5 μm thin, superhydrophilic layer of nanoporous poly(hydroxyethyl methacrylate-*co*-ethylene dimethacrylate) (HEMA-EDMA) was photografted with 2,2,3,3,3-pentafluoropropyl methacrylate (PFPMA) through a quartz chromium photomask to create superhydrophobic regions (see details in the Electronic Supplementary Information†). Using this method, arrays of superhydrophilic spots with specific geometry and size can be created. The superhydrophilic spots can be separated by superhydrophobic barriers with widths as narrow as 50 μm. Photografting occurs through the whole thickness of the porous polymer film, thus there is no mixing of solutions between the superhydrophilic spots.[13] In this work, we used pattern geometries consisting of superhydrophilic circles (3 or 1 mm diameter, 100 μm barrier), triangles (3 or 1 mm side length, 100 μm barrier), hexagons (2 or 1 mm side length, 100 μm barrier), and squares (2 mm, 1 mm, 800 μm, 650 μm, 500 μm, 200 μm, or 100 μm side length, 100 μm barrier; 500 μm side length, 62.5 μm barrier; 335 μm side length, 60 μm barrier).

We show that it is possible to create arrays of thousands of microdroplets in a single step simply by dipping the substrate into an aqueous solution or rolling a droplet across the surface (Fig. 1, Fig. S1† and Video S1†). The rolling droplet method is useful for printing precious reagents because many spots can be filled without using a large amount of solution. Due to the extreme difference in wettability of the superhydrophilic spots compared to the superhydrophobic barriers, water is spontaneously removed from the barriers, but fills the superhydrophilic regions. A similar process is described by Jackman *et al.* as discontinuous dewetting, where the differences in interfacial free energies of the surface and liquid cause an abrupt change in the receding water contact angle (WCA) as liquid moves from the superhydrophilic area to the superhydrophobic barrier.[20] The liquid becomes pinned at the boundary between the superhydrophilic and superhydrophobic areas, and as the liquid continues to move across the barrier, the liquid film thins and eventually separates from the pinned droplet.

Our nanoporous HEMA-EDMA surface which is photografted with PFPMA on a large area possesses static, advancing,

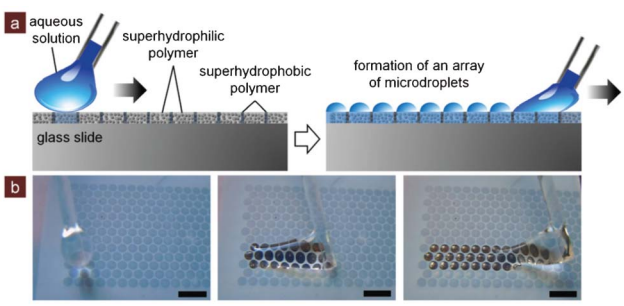

Fig. 1 Formation of a DropletMicroarray using the rolling droplet method. (a) Schematic of a superhydrophilic, nanoporous polymer layer grafted with superhydrophobic moieties. When an aqueous solution is rolled along the surface, the extreme wettability contrast of superhydrophilic spots on a superhydrophobic background leads to the spontaneous formation of a high-density array of completely separated microdroplets. (b) Snapshots of water being rolled along a superhydrophilic–superhydrophobic patterned surface (1 mm diameter circles, 100 μm barrier) to form droplets only in the superhydrophilic spots. Scale bars are 3 mm.

and receding WCAs of 165°, 167°, and 157°, respectively.[13] No separated droplets could be formed on patterned substrates having a low receding WCA on 60 μm-wide hydrophobic barriers (data not published). This demonstrates that automatic formation of densely packed droplets will only occur when there is an extreme difference in the receding WCA between the hydrophilic and hydrophobic areas. In cases where there are insignificant differences between the receding WCAs, the formation of droplets is still possible if the width of the hydrophobic barriers are significantly increased, at the expense of droplet density and hence the throughput.

Examples of arrays of water microdroplets with different geometries and sizes are depicted in Fig. 2a. Formation of droplets in sharp-edged complex geometries, such as triangles, is also possible. As shown in the images, as soon as the nanoporous superhydrophilic areas are wetted, the polymer becomes transparent due to reduced light scattering caused by matched refractive indexes, allowing easier discrimination of spots and facilitating the use of inverted microscopes. Each microdroplet functions as a small lens with the surface curvature determined by the geometry of the superhydrophilic spot (Fig. 2b).

The volumes of the individually formed droplets depend on the size and geometry of the superhydrophilic spots, as well as on the surface tension of the solution (Fig. S2†), and can be controlled between 700 pl and 3 μl for the patterns we tested (Fig. 3a and ESI†). Thus, an array of 85 000 700 pl microdroplets can be easily formed in a matter of seconds on a microtiter plate-sized glass slide prepatterned with 200 × 200 μm^2 superhydrophilic squares separated by 100 μm wide superhydrophobic barriers. Approximately fifty-five 1536-well plates would be needed for the equivalent of 85 000 wells. It should be noted that although droplet microfluidics provides comparable or even higher throughput, the addressability of the droplets surrounded by oil and located inside microfluidic channels is significantly more difficult than that of droplets positioned in defined X,Y locations on the surface of the DropletMicroarray.

To determine if the volumes of the droplets are homogeneous and reproducible, square patterns (500 μm side length, 62.5 μm barriers) were dipped into Rhodamine 6G water solutions to create an array of 8 nl microdroplets, dried, and then imaged to measure the fluorescent intensities. Three different concentrations of Rhodamine 6G were tested (0.1, 0.05, and 0.025 mg ml^{-1}), and for each concentration three different substrates were measured. Multiple images were taken of each substrate. Fig. 3b shows an example of the selected regions of interest (ROI), and Fig. 3c compares the intensity profile from one sample at each of the three different Rhodamine 6G concentrations. The fluorescent intensities are relatively equal across each sample, and the intensity increases with the Rhodamine 6G concentration. The slight variability of the Rhodamine 6G intensity within each square is probably due to the nature of the rough polymer surface. When the fluorescent intensity within each square was averaged over all three samples for each Rhodamine concentration, there was low variability in the measurements (Fig. 3d). The mean fluorescent intensities were 154 ± 2.2%, 121 ± 1.8%, 91.0 ± 0.42%, and 6.09 ± 0.35% for Rhodamine 6G concentrations of 0.1, 0.05, 0.025, and 0 mg ml^{-1}, respectively. This indicates that the formation of isolated droplets on our superhydrophilic–superhydrophobic polymer surface is reproducible and results in

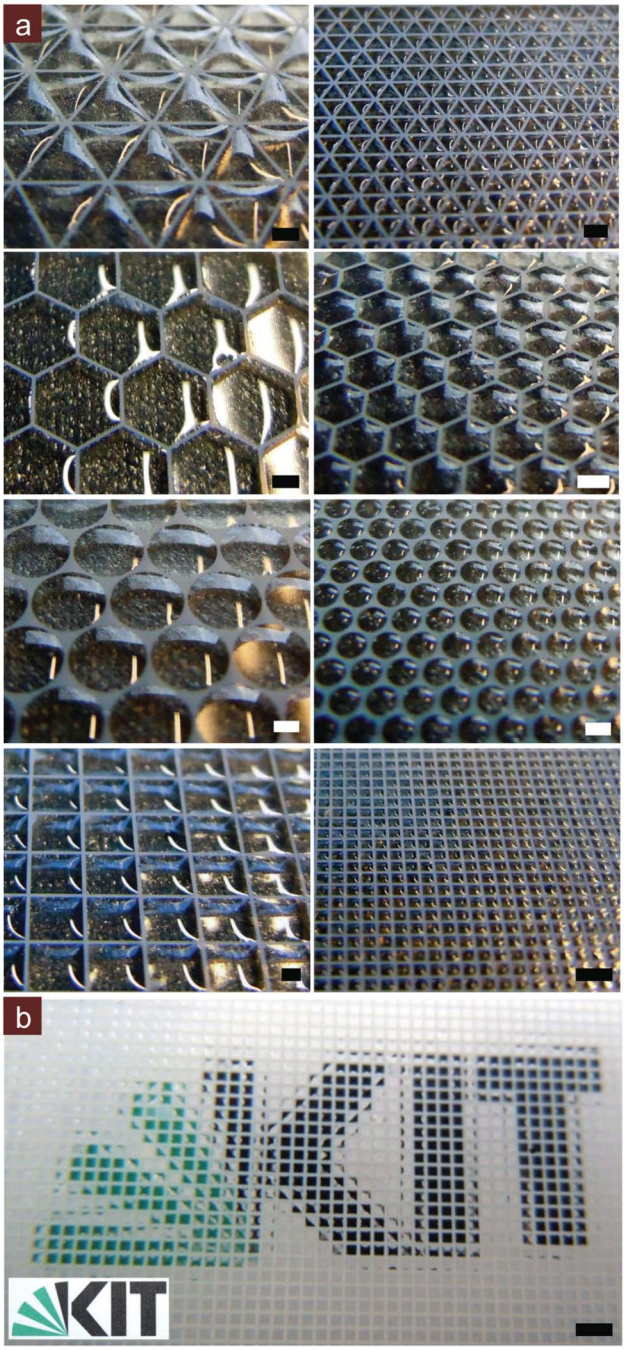

Fig. 2 (a) DropletMicroarrays formed by dipping the superhydrophilic–superhydrophobic patterns of different geometries into water. (b) The wetted superhydrophilic–superhydrophobic micropattern becomes transparent and displays a lens effect, showing the underlying logo. Scale bars are 1 mm.

low variability of the individual droplet volumes. This variability is comparable to what is achievable with optimized parameters in EWOD devices, which can have variance coefficients as low as 2%.[19]

With such small droplet volumes and large surface-to-volume ratios, methods to prevent evaporation of the droplets are critical. High humidity (~80% RH) environments can slow evaporation, but we also found that Petri dishes, which were

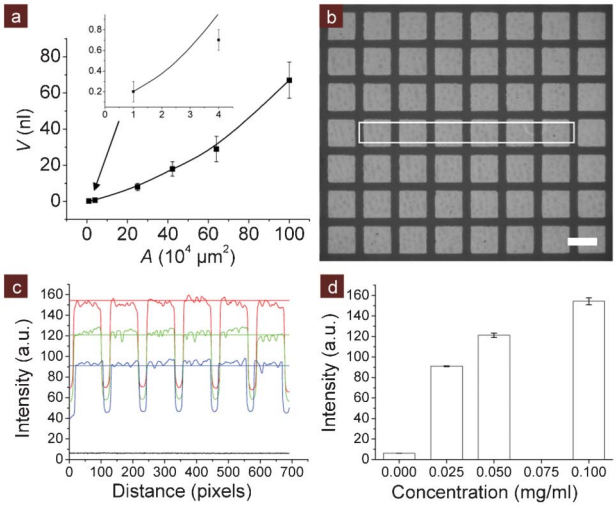

Fig. 3 Individual droplet volume quantification and reproducibility. (a) Influence of the superhydrophilic spot area (A) on the average water droplet volume (V) confined in a single spot of square geometry (100 µm superhydrophobic barriers for all patterns). Inset zooms in on the first two data points. This data is available in Table S2.† (b) An example of a ROI selected to quantify droplet reproducibility. Grayscale image shows 0.1 mg ml^{-1} Rhodamine 6G deposited on an array of superhydrophilic squares (500 µm side length, 62.5 µm barrier) after drying in air. Scale bar is 500 µm. (c) The fluorescent intensity profile of six squares (500 µm side length, 62.5 µm barrier) from a representative sample for 3 different concentrations of Rhodamine 6G: 0.1 mg ml^{-1} (red), 0.05 mg ml^{-1} (green), 0.025 mg ml^{-1} (blue), and 0 mg ml^{-1} (black). The horizontal line is the mean fluorescent intensity across the triplicates, analyzed for each Rhodamine 6G concentration (also shown in 3d). (d) The mean Rhodamine 6G fluorescent intensity in the superhydrophilic spots across the triplicates analyzed for each Rhodamine 6G concentration. Error bars are ± standard deviation.

pre-humidified such that condensation formed on the lids, were able to inhibit evaporation of 8 nl water droplets formed on a pattern of squares (500 µm side length, 62.5 µm barriers) for at least 8 h when kept in a room at ambient conditions (28 °C, 40% RH). Surrounding the substrate with drops of PBS instead of water also seemed to slow evaporation. In an incubator where it is much more humid, longer incubation times for cells, of at least 24 h, are possible. Alternatively, the droplets can be covered with a layer of immiscible oil that is permeable to air.

Encapsulation of cells in arrays of microdroplets

The formation of DropletMicroarrays on the superhydrophilic–superhydrophobic nanoporous polymer substrate can be used as a rapid and convenient tool for the patterning of chemicals, particles, cells, or any other components present in an aqueous solution. Fig. 4a shows an array of microdroplets containing human cervical tumor cells stably expressing green fluorescent protein (HeLa-GFP) 18 h after droplet formation on a square pattern (500 µm side length, 62.5 µm barriers). The brightfield images show that the droplets have not evaporated, while the fluorescent images show that cells were present in each droplet on the array and no cells were present on the superhydrophobic barriers. This type of array combines the features of microplates, where cells present in individual wells are physically isolated

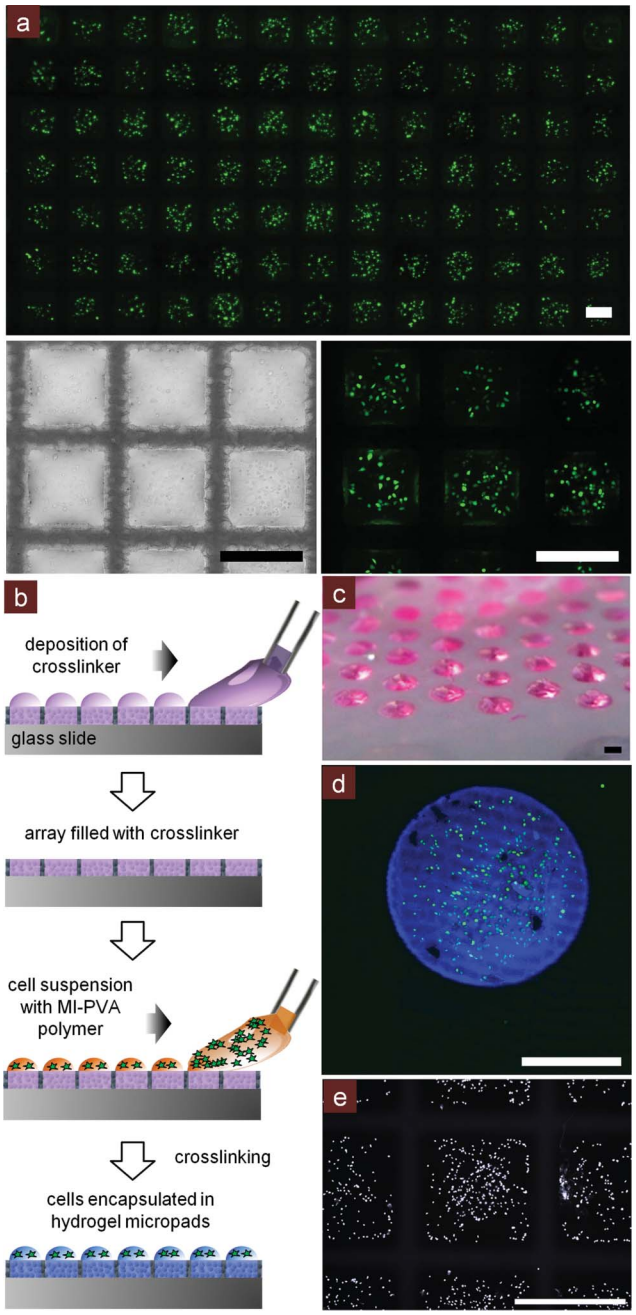

Fig. 4 Encapsulation of cells in arrays of microdroplets and hydrogel micropads. (a) Fluorescent HeLa-GFP cells cultured in individual microdroplets for 18 h. (b) Schematic showing the formation of arrays of hydrogel micropads incorporating cells. First, PEG-crosslinker is deposited in the superhydrophilic spots using the rolling droplet method and then dried in air. Then, a cell suspension mixed with MI-PVA is deposited using the rolling droplet method and crosslinking occurs to form separated hydrogel micropads encapsulating cells. (c) Hydrogel micropads stained with Rhodamine 6G, in air. (d) Fluorescent HT1080-eGFP cells encapsulated in hydrogel micropads stained with 7-diethylamino-3-(4-maleimidophenyl)-4-methylcoumarin (blue) for gel visualization after hydrogel crosslinking and immersion in the medium. Cells remain contained within the hydrogel. (e) Fixed and DAPI-stained (white) lt-NES cells encapsulated in hydrogel micropads at day 6. Brightfield images in Fig. S4.† Scale bars are 500 μm.

from each other, with the advantages of miniaturization and parallelization of cell microarrays used for reverse cell transfection.

As opposed to droplet microfluidics, superhydrophilic spots on a DropletMicroarray can be directly pre-printed with libraries of small molecules or transfection reagents using a conventional contact or non-contact microprinter. The diffusion of small molecules will be confined to the individual microdroplets, which in turn can save a lot of precious materials and prevent inter-spot mixing. DropletMicroarrays allow the rapid formation of thousands of droplets of any tailored geometry or arrangement and the encapsulation of microorganisms. A disadvantage is that the small volume of the microdroplets limits the number of cells or time that cells can be cultured inside individual droplets to avoid nutrient starvation. For the 500 μm side length square pattern that forms droplets of approximately 8 nl, a single cell per droplet is equivalent to a cell concentration of 125 000 cells ml^{-1}. In a Petri dish with a confluent layer of cells, the cell concentration can be around 1 million cells ml^{-1}. This suggests that multiple cell divisions of a single cell or several cells cultured for a shorter time in the droplet would be acceptable. This limitation could also be overcome by optimizing the culture medium, or using inkjet printers, piezoelectric dispensers, or microfluidic devices to exchange medium in the droplets. Nevertheless, this one-step formation of thousands of microdroplets incorporating cells or other biological species can be useful for a variety of screening applications.

Encapsulation of cells in arrays of hydrogel micropads

Culturing cells in 3D microenvironments, such as hydrogels, *versus* 2D cell cultures has been shown to more closely mimic the *in vivo* situation.[16] It was also shown that cell behavior in a 3D microenvironment can be different from the behavior of cells cultured on flat surfaces.[15] Therefore, HT screening of cells in 3D systems is an important challenge that is yet to be fully realized.

We demonstrate the applicability of the DropletMicroarray for creating arrays of hydrogel micropads incorporating cells. Fig. 4b schematically shows the process of formation of an array of hydrogel micropads. In the first step, a poly(ethylene glycol) crosslinker bearing two thiol groups (PEG-crosslinker) is printed into the superhydrophilic microspots by rolling a droplet across the surface, and then dried. In the next step, an array of microdroplets containing a solution of maleimide-functionalized polyvinyl alcohol (MI-PVA) and cells is created using the rolling droplet method. The thiol groups in the PEG-crosslinker form thioether bonds with the maleimide groups in the MI-PVA and crosslink the polymer to form a stable, biocompatible hydrogel within minutes in which living and nonadherent cells can be trapped. Thus, only two steps and several minutes are necessary to create an array of up to 85 000 hydrogel micropads for performing high-throughput cell screening.

After the hydrogel is formed, the array of hydrogel micropads incorporating cells can be immersed in the cell culture medium, or droplets of the medium can be formed in the superhydrophilic spots to isolate each hydrogel micropad for further culturing. Fig. 4c shows an array of hydrogel micropads in air that have been incorporated with Rhodamine 6G dye for visibility. In

addition, live cells (HT1080-eGFP human fibrosarcoma cells and long-term self-renewing neuroepithelial-like stem cells (lt-NES cells) derived from hESC lines H9) were encapsulated and distributed throughout the hydrogel micropads and imaged after hydrogel formation and six days, respectively (Fig. 4d,e, S3, and S4† and video S2†).[21] Incorporating the thiol-reactive probe, 7-diethylamino-3-(4-maleimidophenyl)-4-methylcoumarin, in the PEG-crosslinker mixture allows us to visualize successful crosslinking of the gel since it only fluoresces when it reacts with the thiol groups on maleimide. Fig. 4d and S3† confirm that hydrogels were only formed within the superhydrophilic spots and no cells were observed outside the gel. Fig. 4e also demonstrates that no cells lie on the superhydrophobic barriers and are immobilized by the hydrogel in the superhydrophilic spots. The fluorescent HT1080-eGFP cells (Fig. 4d) can be visualized starting from the top to the bottom of the hydrogel in a 196 μm z-stack obtained using a confocal microscope (Video S2†).

The two-step procedure introduced here to form hydrogels encapsulating cells in about 5 min is simple enough to be used for screening cells in 3D hydrogels. In principle, our superhydrophilic–superhydrophobic polymer substrate is compatible with other methods for forming hydrogels, provided the surface tension of the pre-hydrogel mixture is high enough. For example, UV-initiated curing of gelatin methacrylate[22,23] or PEG diacrylate,[23,24] or ionic crosslinking of alginate-based hydrogels[25–28] could be potentially formed on our substrate according to the referenced methods. For our method presented here, the MI-PVA hydrogel was especially appealing because it is a facile and quick method, gentle in terms of cell handling, and does not require exposing cells to UV light. In addition, the MI-PVA hydrogel can be easily incorporated with, for example, adhesive peptides such as RGD, other ECM motifs, signalling molecules, drugs, or other small molecules for 3D cell screenings.

Doxorubicin cytotoxicity screen using 3D hydrogel micropads

As a proof-of-concept of the application of arrays of hydrogel micropads for cell screening, we performed a cytotoxicity test by exposing human breast adenocarcinoma cells (MDA-MB-231) to doxorubicin, a chemotherapeutic drug known to induce apoptosis. Decreasing amounts of doxorubicin (25, 20, 15, 10, 5, and 2.5 ng) and a water control were pre-printed in superhydrophilic spots of a circular pattern (1 mm diameter, 500 μm superhydrophobic barriers). MI-PVA hydrogel micropads encapsulating MDA-MB-231 cells were formed in these spots and briefly immersed in the medium to swell the hydrogel, and then removed from the medium to isolate each hydrogel micropad during incubation. After 18 h of incubation, the cells in the hydrogel micropads were stained with Calcein AM and propidium iodide (PI) to quantify live and dead cells, respectively.

The percentage of apoptotic cells exhibited a dose-dependency on the amount of pre-printed doxorubicin. The percentage of Calcein AM-positive cells decreased while the percentage of PI-positive cells increased with increasing amounts of pre-printed doxorubicin (Fig. 5). This demonstrates that doxorubicin was able to diffuse from the substrate into the hydrogel over the 18 h incubation time and induce apoptosis, and the hydrogel micropads were isolated such that no apparent mixing of doxorubicin and the water control was observed. This simple example shows the feasibility of screening cells in hydrogel micropads.

In terms of non-destructive bioassays, the hydrogel micropads are compatible with mainly live-cell imaging, monitoring fluorescent reporter genes, or immunofluorescent staining, and possibly enzymatic or colorimetric assays. The superhydrophobic barriers can contain different solutions in each superhydrophilic spot, thus different probes can be deposited and incubated on each spot. The main limitation against performing bioassays is washing of individual micropads without mixing. Destructive bioassays, such as Western blotting, may be possible since the hydrogel micropads containing cells can be physically addressed from outside, removed, and further degraded.

Materials and methods

All polymerizations and photografting were carried out on an OAI Model 30 deep-UV collimated light source (San Jose, CA)

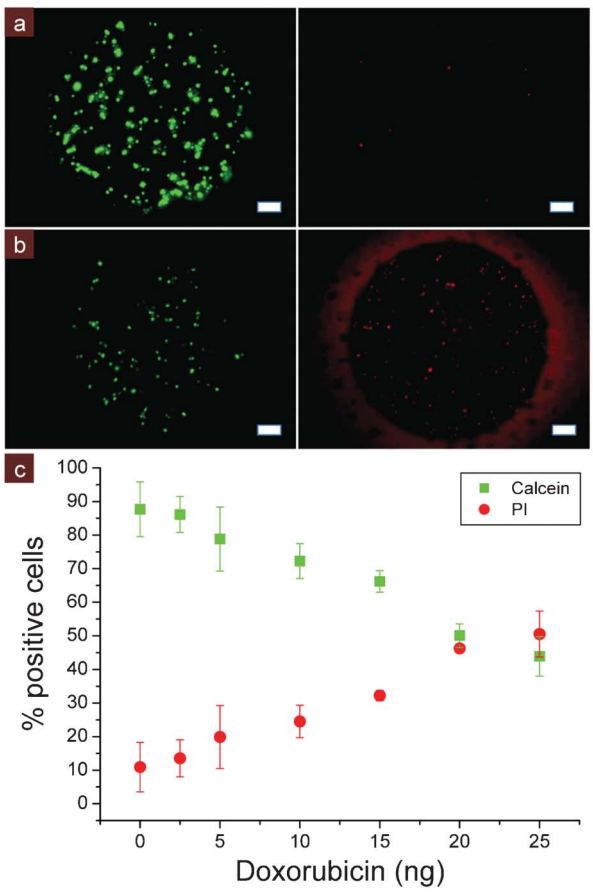

Fig. 5 Doxorubicin cytotoxicity screen using hydrogel micropads encapsulating MDA-MB-231 cells. After 18 h of incubation, cells were stained with Calcein AM (green) and propidium iodide (PI) (red). (a) Stained cells in hydrogel micropad on a spot pre-printed with water control. (b) Stained cells in hydrogel micropad on a spot pre-printed with 25 ng of doxorubicin. Scale bars are 100 μm. Fluorescent intensity has been enhanced for visualization. (c) Mean percentage of Calcein AM and PI-positive cells per hydrogel micropad for each amount of pre-printed doxorubicin after 18 h of incubation. Error bars are ± standard deviation.

fitted with an USHIO 500 W Hg-xenon lamp (Japan). Irradiation intensity was calibrated to 12 mW cm^{-2} (5.10 mW cm^{-2} after cover glass slide, 4.77 mW cm^{-2} after cover glass slide and photomask) using an OAI 360 UV power meter with a 260 nm probe head. Schott (Germany) Nexterion Glass B UV transparent glass plates were used as substrates for polymer layers. Monomers were purchased from Sigma-Aldrich (Germany). Biochemicals were purchased from Life Technologies (Germany). HeLa-GFP cells were purchased from Biocat (Germany). HT1080-eGFP and MDA-MB-231 cells were provided by the Institute of Toxicology and Genetics at Karlsruhe Institute of Technology. Long-term self-renewing neuroepithelial-like stem cells (lt-NES cells) derived from hESC lines H9 were generously provided by Dr Philipp Koch at the University of Bonn. Hydrogels were made using the 3-D Life PVA-PEG Hydrogel Kit from Cellendes GmbH (Germany).

Quantification of the reproducibility of individual droplet volumes

Substrates were dipped into a Rhodamine 6G water solution (0.1 mg ml^{-1}, 0.05 mg ml^{-1}, or 0.025 mg ml^{-1}) for 5 s, removed to form a DropletMicroarray, and then dried in air. Patterns were imaged on a Leica MZ10 F widefield microscope (2.5× zoom, 2.47 ms exposure time) at three locations per sample and three samples per Rhodamine 6G concentration. Fluorescent intensity was quantified using ImageJ. ROI spanning six squares were selected on the images acquired for three different concentrations and the intensity profiles were plotted. To calculate the mean intensity and standard deviation over all three samples for each Rhodamine 6G concentration, many ROI within single squares were selected and the mean intensity of each histogram was measured to calculate the mean intensity and standard deviation across all three samples for each Rhodamine 6G concentration.

Hydrogel array formation

The 3-D Life PVA-PEG Hydrogel Kit from Cellendes GmbH (Germany) was used. For hydrogel visualization, the crosslinker solution was prepared by mixing 23 µl PEG-crosslinker + 2 µl of 1 mg ml^{-1} 7-diethylamino-3-(4-maleimidophenyl)-4-methylcoumarin in DMSO. Otherwise, just 25 µl of PEG-crosslinker was used. The patterned substrate was placed in a Petri dish. A pipette was used to roll the 25 µl of crosslinker solution across the patterned substrate. Only the hydrophilic spots were wetted with the crosslinker solution. The crosslinker solution was dried. The MI-PVA cell solution was prepared such that the final concentration of MI was 6 mM: 12.5 µl water + 2.5 µl 10X CB pH 5.5 buffer + 5 µl MI-PVA (30 mM MI stock) + 5 µl of 80 × 10^6 cells ml^{-1} cell suspension. A pipette was used to roll the 25 µl of MI-PVA-cell solution across the patterned substrate where the crosslinker solution was printed. This was done quickly and if available under humid conditions to prevent the gel from drying out. Droplets of the medium or PBS were dispensed around the substrate and then put in a humidified incubator until the polymerization was finished (about 5 min). The hydrogel–cell array was then immersed in the medium. See Video S2† to visualize the fluorescent HT1080-eGFP cells (Fig. 4d) starting from the top to the bottom of the hydrogel in a 196 µm z-stack obtained using a Leica TCS SP5 confocal microscope.

Doxorubicin cytotoxicity screen

Doxorubicin solutions (50, 40, 30, 20, 10, and 5 µg ml^{-1} in water) and a water control were pipetted in a row at 0.5 µl each in the superhydrophilic spots of a circle patterned substrate (1 mm diameter, 500 µm barrier). Three replicate rows were printed on each of the two different substrates. MI-PVA hydrogel micropads encapsulating MDA-MB-231 cells were formed as described above on the pre-printed spots, but instead using 5 µl of 20 × 10^6 cells ml^{-1} cell suspension. After the hydrogel was crosslinked in 5 min, the substrate was immersed in the medium for 1 min to swell the hydrogel and then removed from the medium to isolate each hydrogel micropad during incubation. After 18 h of incubation, the cells in the hydrogel micropads were washed twice with PBS, stained with 0.5 µM Calcein AM, 500 nM PI, and 1 µg ml^{-1} Hoechst 33342 for 20 min, rinsed once with PBS, and imaged as z-stacks on a Keyence BZ-9000 fluorescent microscope (Japan). The images were quantified in ImageJ using the Cell Counter plugin. All other procedures are explained in detail in the ESI.†

Conclusions

We developed a facile and rapid method to fabricate microarrays of separated, spatially organized droplets with controlled position, geometry, and volume on a superhydrophilic, nanoporous polymer surface patterned with superhydrophobic moieties. The droplets can encapsulate any substance dissolved or suspended in an aqueous solution, and drying the droplets results in the homogeneous deposition of the substance in the superhydrophilic microspots.

The droplet deposition method can also be used to form arrays of hydrogel micropads incorporating cells. Nonadherent cells or other microbiological species (amoeba, bacteria, yeast) can easily be immobilized in a high-density 3D array and used for biological screens. The small volumes of the droplets require fewer reagents compared to microplates and can enhance the detection of low abundance molecules or signals. The DropletMicroarray does not rely on physical barriers to separate the droplets, so the glass slides can be coverslipped if needed.

As opposed to droplet microfluidics where screenings of large libraries of molecules are difficult to perform in the droplets, DropletMicroarrays are compatible with both automated contact and noncontact printing techniques, thus combining the advantages of microarray technology and the HT compartmentalization abilities of droplet microfluidics. In combination with automated printing techniques, the droplets can be individually addressed or exactly a single cell can be cultured in each droplet.[29] Our superhydrophilic–superhydrophobic surfaces could also be combined with technologies such as digital microfluidics to have full control of the liquid movement across the surface and thus droplet formation.[30,31] It would also be possible to use our superhydrophilic–superhydrophobic surfaces to create crystal[32] or protein arrays upon evaporation of droplets.

We envision DropletMicroarrays to be an important step towards the development of HT screening platforms that are practical and adaptable to screening nonadherent or single cells and 3D cell microenvironments with large libraries of molecules,

such as drug candidates or nucleic acids. Currently, we are working towards several applications of this novel technology.

Acknowledgements

We are grateful to the Helmholtz Association's Initiative and Networking Fund (Grant VH-NG-621) and the Department of Applied Physical Chemistry at Heidelberg University (Prof. M. Grunze) for the financial support. We are grateful to Dr Philipp Koch at the University of Bonn for generously providing the long-term self-renewing neuroepithelial-like stem cells (lt-NES cells) derived from hESC lines H9.

References

1 R. A. Lindquist, K. A. Ottina, D. B. Wheeler, P. P. Hsu, C. C. Thoreen, D. A. Guertin, S. M. Ali, S. Sengupta, Y. D. Shaul, M. R. Lamprecht, K. L. Madden, A. R. Papallo, T. R. Jones, D. M. Sabatini and A. E. Carpenter, *Genome Res.*, 2011, **21**, 433–446.
2 K. C. Wood, D. J. Konieczkowski, C. M. Johannessen, J. S. Boehm, P. Tamayo, O. B. Botvinnik, J. P. Mesirov, W. C. Hahn, D. E. Root, L. A. Garraway and D. M. Sabatini, *Sci. Signaling*, 2012, **5**, rs4–rs4.
3 D. J. Siegwart, K. A. Whitehead, L. Nuhn, G. Sahay, H. Cheng, S. Jiang, M. Ma, A. Lytton-Jean, A. Vegas, P. Fenton, C. G. Levins, K.T. Love, H. Lee, C. Cortez, S. P. Collins, Y. F. Li, J. Jang, W. Querbes, C. Zurenko, T. Novobrantseva, R. Langer and D. G. Anderson, *Proc. Natl. Acad. Sci. U. S. A.*, 2011, **108**, 12996–3001.
4 D. A. Brafman, S. Chien and K. Willert, *Nat. Protoc.*, 2012, **7**, 703–717.
5 J. Ziauddin and D. M. Sabatini, *Nature*, 2001, **411**, 107.
6 S. Mousses, N. J. Caplen, R. Cornelison, D. Weaver, M. Basik, S. Hautaniemi, A. G. Elkahloun, R. A. Lotufo, A. Choudary, E. R. Dougherty, E. Suh and O. Kallioniemi, *Genome Res.*, 2003, **13**, 2341–2347.
7 S. Baghdoyan, Y. Roupioz, A. Pitaval, D. Castel, E. Khomyakova, A. Papine, F. Soussaline and X. Gidrol, *Nucleic Acids Res.*, 2004, **32**, e77–e77.
8 H. Erfle, B. Neumann, U. Liebel, P. Rogers, M. Held, T. Walter, J. Ellenberg and R. Pepperkok, *Nat. Protoc.*, 2007, **2**, 392–399.
9 M. Stürzl, A. Konrad, G. Sander, E. Wies, F. Neipel, E. Naschberger, S. Reipschläger, N. Gonin-Laurent, R. E. Horch, U. Kneser, W. Hohenberger, H. Erfle and M. Thurau, *Comb. Chem. High Throughput Screening*, 2008, **11**, 159–172.
10 A. L. Hook, H. Thissen and N. H. Voelcker, *Biomacromolecules*, 2009, **10**, 573–579.
11 A. I. Neto, C. A. Custódio, W. Song and J. F. Mano, *Soft Matter*, 2011, **7**, 4147.
12 J. K. Rantala, R. Mäkelä, A.-R. Aaltola, P. Laasola, J.-P. Mpindi, M. Nees, P. Saviranta and O. Kallioniemi, *BMC Genomics*, 2011, **12**, 162.
13 F. L. Geyer, E. Ueda, U. Liebel, N. Grau and P. A. Levkin, *Angew. Chem., Int. Ed.*, 2011, **50**, 8424–8427.
14 S. Lindström and H. Andersson-Svahn, *Lab Chip*, 2010, **10**, 3363–72.
15 F. Pampaloni, E. G. Reynaud and E. H. K. Stelzer, *Nat. Rev. Mol. Cell Biol.*, 2007, **8**, 839–45.
16 A. Skardal, L. Smith, S. Bharadwaj, A. Atala, S. Soker and Y. Zhang, *Biomaterials*, 2012, **33**, 4565–75.
17 A. Huebner, D. Bratton, G. Whyte, M. Yang, A. J. Demello, C. Abell and F. Hollfelder, *Lab Chip*, 2009, **9**, 692–8.
18 C. H. J. Schmitz, A. C. Rowat, S. Köster and D. A. Weitz, *Lab Chip*, 2009, **9**, 44–9.
19 N. Vergauwe, D. Witters, Y. T. Atalay, B. Verbruggen, S. Vermeir, F. Ceyssens, R. Puers and J. Lammertyn, *Microfluid. Nanofluid.*, 2011, **11**, 25–34.
20 R. J. Jackman, D. C. Duffy, E. Ostuni, N. D. Willmore and G. M. Whitesides, *Anal. Chem.*, 1998, **70**, 2280–7.
21 P. Koch, T. Opitz, J. A. Steinbeck, J. Ladewig and O. Brüstle, *Proc. Natl. Acad. Sci. U. S. A.*, 2009, **106**, 3225–30.
22 J. W. Nichol, S. T. Koshy, H. Bae, C. M. Hwang, S. Yamanlar and A. Khademhosseini, *Biomaterials*, 2010, **31**, 5536–5544.
23 H. Qi, Y. Du, L. Wang, H. Kaji, H. Bae and A. Khademhosseini, *Adv. Mater.*, 2010, **22**, 5276–5281.
24 M. J. Hancock, F. Yanagawa, Y. Jang, J. He, N. N. Kachouie, H. Kaji and A. Khademhosseini, *Small*, 2012, **8**, 393–403.
25 T. G. Fernandes, S. Kwon, S. S. Bale, M. Lee, M. M. Diogo, D. S. Clark, J. M. S. Cabral and J. S. Dordick, *Biotechnol. Bioeng.*, 2010, **106**, 106–118.
26 S. A. Zawko and C. E. Schmidt, *Lab Chip*, 2010, **10**, 379–383.
27 W. Song, A. C. Lima and J. F. Mano, *Soft Matter*, 2010, **6**, 5868–71.
28 C. L. Salgado, M. B. Oliveira and J. F. Mano, *Integr. Biol.*, 2012, **4**, 318–27.
29 A. Yusof, H. Keegan, C. D. Spillane, O. M. Sheils, C. M. Martin, J. J. O'Leary, R. Zengerle and P. Koltay, *Lab Chip*, 2011, **11**, 2447–54.
30 I. Barbulovic-Nad, S. H. Au and A. R. Wheeler, *Lab Chip*, 2010, **10**, 1536.
31 D. Witters, N. Vergauwe, S. Vermeir, F. Ceyssens, S. Liekens, R. Puers and J. Lammertyn, *Lab Chip*, 2011, **11**, 2790–4.
32 D. Witters, N. Vergauwe, R. Ameloot, S. Vermeir, D. De Vos, R. Puers, B. Sels and J. Lammertyn, *Adv. Mater.*, 2012, **24**, 1316–20.

